

# Formation of low charge state ions of synthetic polymers using quaternary ammonium compounds

*Andreas Nasioudis<sup>1</sup>; William F. Joyce<sup>2</sup>; Jan W. van Velde<sup>1</sup>; Ron M.A. Heeren<sup>3</sup>; Oscar F. van den Brink<sup>1, \*</sup>*

<sup>1</sup>AkzoNobel Research Development & Innovation, Deventer, The Netherlands; <sup>2</sup>AkzoNobel Surface Chemistry LLC, Brewster, NY, USA; <sup>3</sup>FOM Institute for Atomic and Molecular Physics, Amsterdam, The Netherlands

## SUPPORTING INFORMATION

Figures S-1 to S-7

Tables S-1, S-2

\*To whom correspondence should be addressed. Email: [Oscar.vandenBrink@akzonobel.com](mailto:Oscar.vandenBrink@akzonobel.com) Phone: +31-570-679131. Fax: +31-570-679851

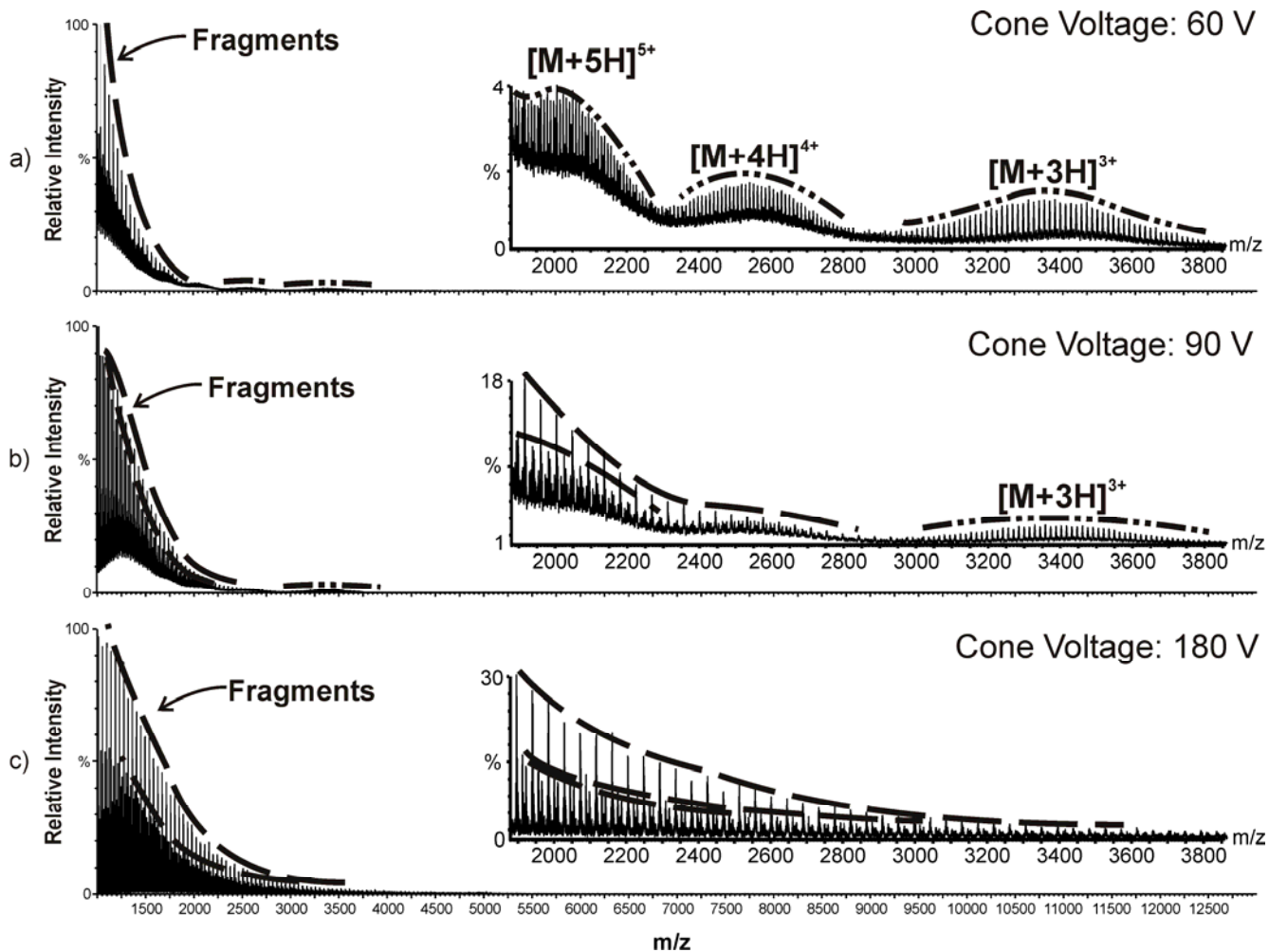


**Figure S-1.** Mass spectra of 10 kDa PEG obtained by direct infusion without addition of a Quat at different cone voltage values: a) 60 V, b) 90 V and c) 180 V. Note: Inset figures are a magnification of the area of interest in Figures S-1a, S-1b and S-1c.

The increase of cone voltage induces up-front fragmentation of the protonated PEG ions

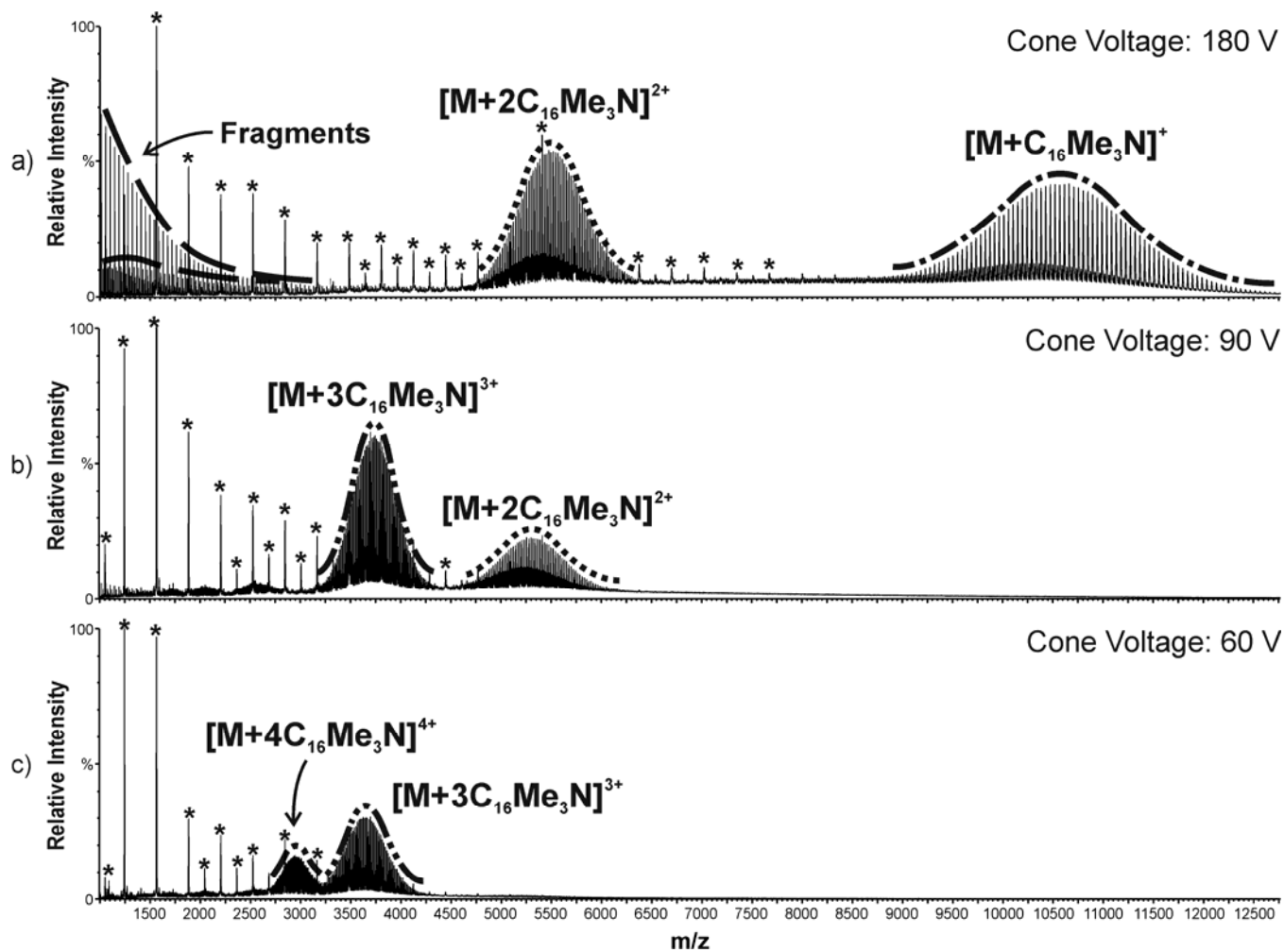


**Figure S-2.** Mass spectra of 10 kDa PEG obtained by direct infusion with addition of 1.2 mM  $C_{16}Me_3NCl$  at different cone voltage values: a) 180 V, b) 90 V and c) 60 V.

The decrease of cone voltage value results in the formation of higher charge state  $[PEG+nC_{16}Me_3N]^{n+}$  ions (n is 2 to 4) and the disappearance of the protonated fragment ions.

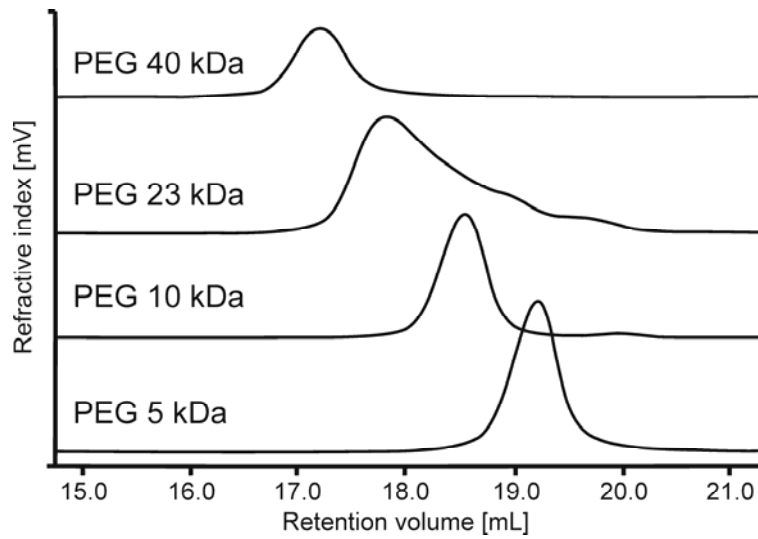


**Figure S-3.** SEC analysis of various PEGs. Overlaid Refractive index (RI) chromatograms of 5, 10, 23 and 40 kDa PEG. Note: Ordinate has an arbitrary scale.

From the RI chromatograms, it is observed that all PEGs except the PEG 23 kDa are relatively monodisperse.

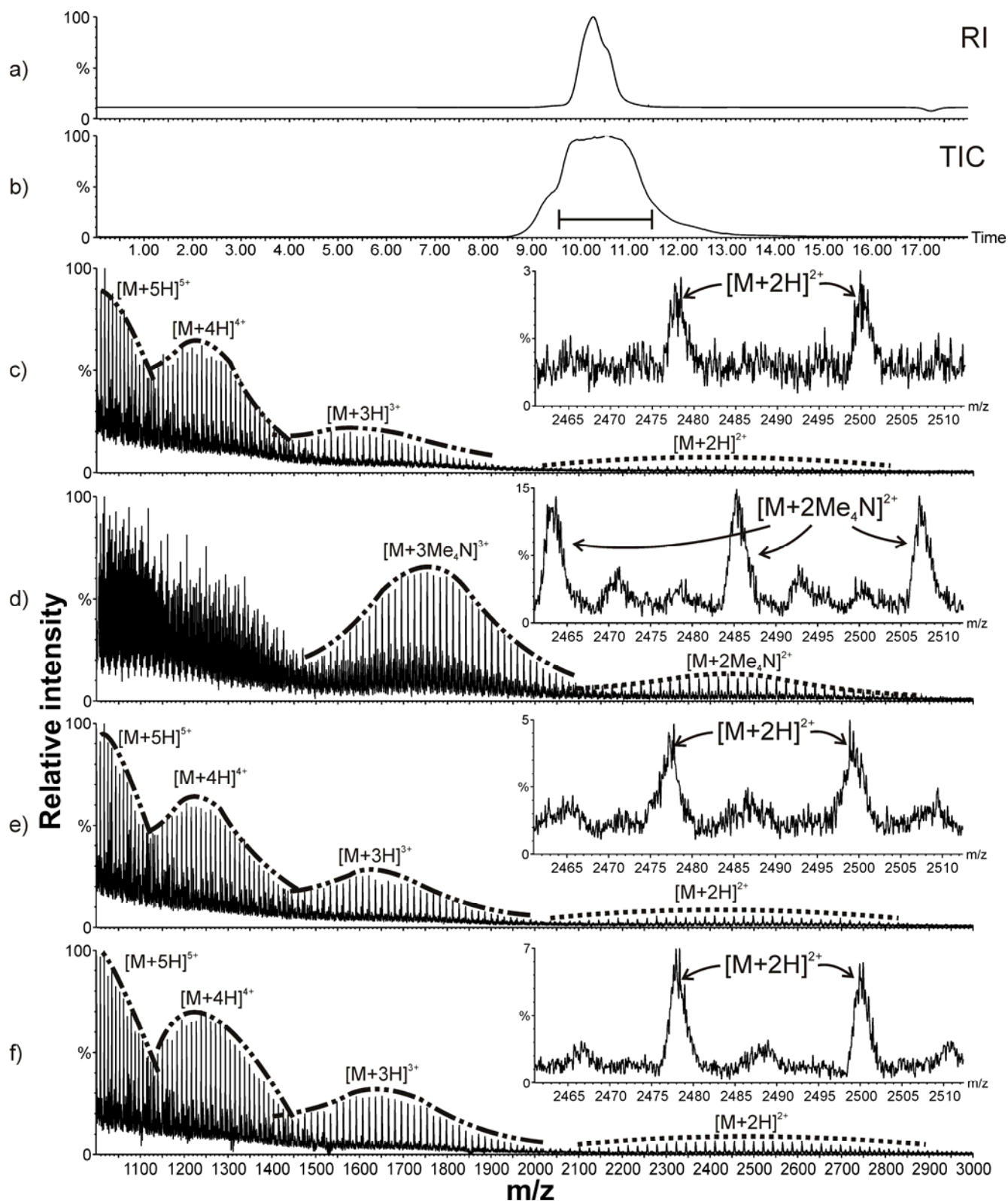


**Figure S-4.** SEC-MS of 5 kDa PEG. Influence of the substituent size on the charge state reduction performance: a) RI signal, b) Total ion count (TIC) signal and c), d), e) and f) are summed mass spectra of the main TIC peak of: c) no Quat (Blank), d) Me<sub>4</sub>NCl, e) Et<sub>4</sub>NCl and f) Bu<sub>4</sub>NCl. Note: All mass spectra are obtained in the same ESI conditions. Inset figures are a magnification of the area of interest in Figures S-4c, S-4d, S-4e, and S-4f.

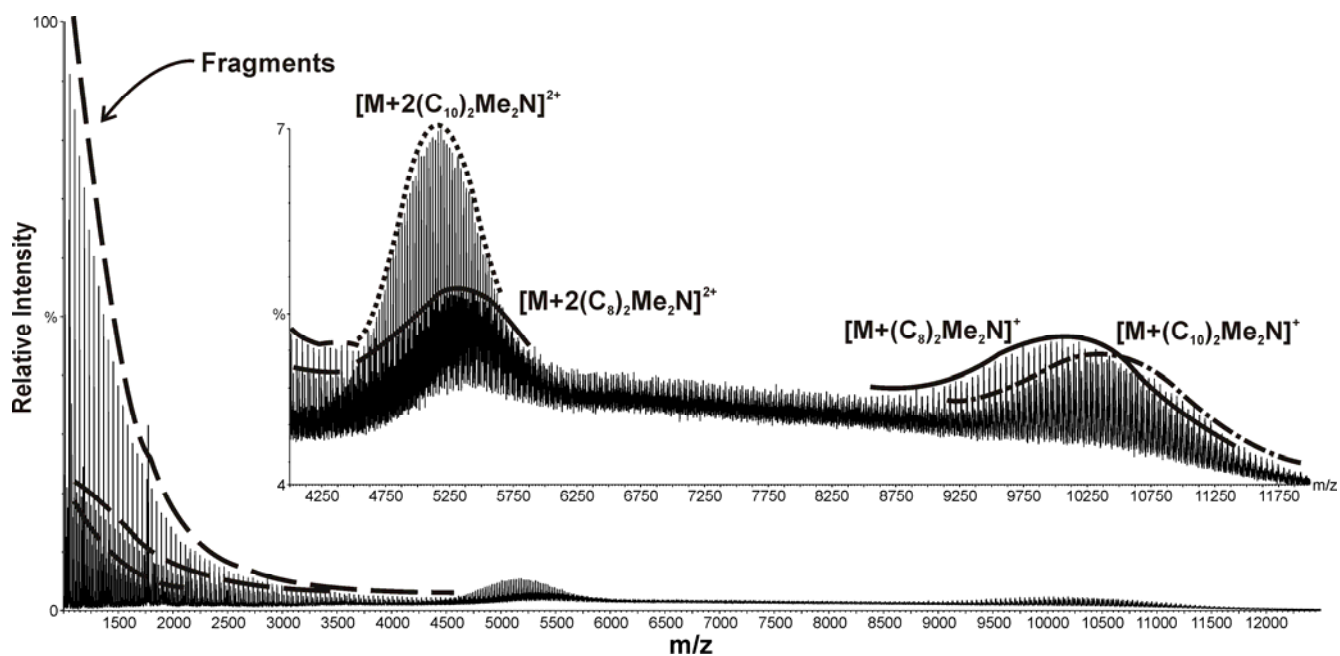


**Figure S-5.** Mass spectra of 10 kDa PEG obtained by direct infusion with addition of 1.2 mM  $(C_{10})_2Me_2NCl$ . Note: The presence of  $[M+n(C_8)_2Me_2N]^{n+}$  ions are expected, because  $(C_{10})_2Me_2NCl$  sample is not pure and contains  $(C_8)_2Me_2NCl$ . Inset figure is a magnification of the area of interest in Figure S-5.

Although Quats with two long alkyl chains coordinate with PEG chains, their intensity is much lower than the protonated PEG fragment ions. A comparison can be made with Figure S-2a, where in the same ESI conditions the  $[PEG+C_{16}Me_3N]^+$  ions have a comparable intensity with the  $[PEG+H]^+$  fragment ions.

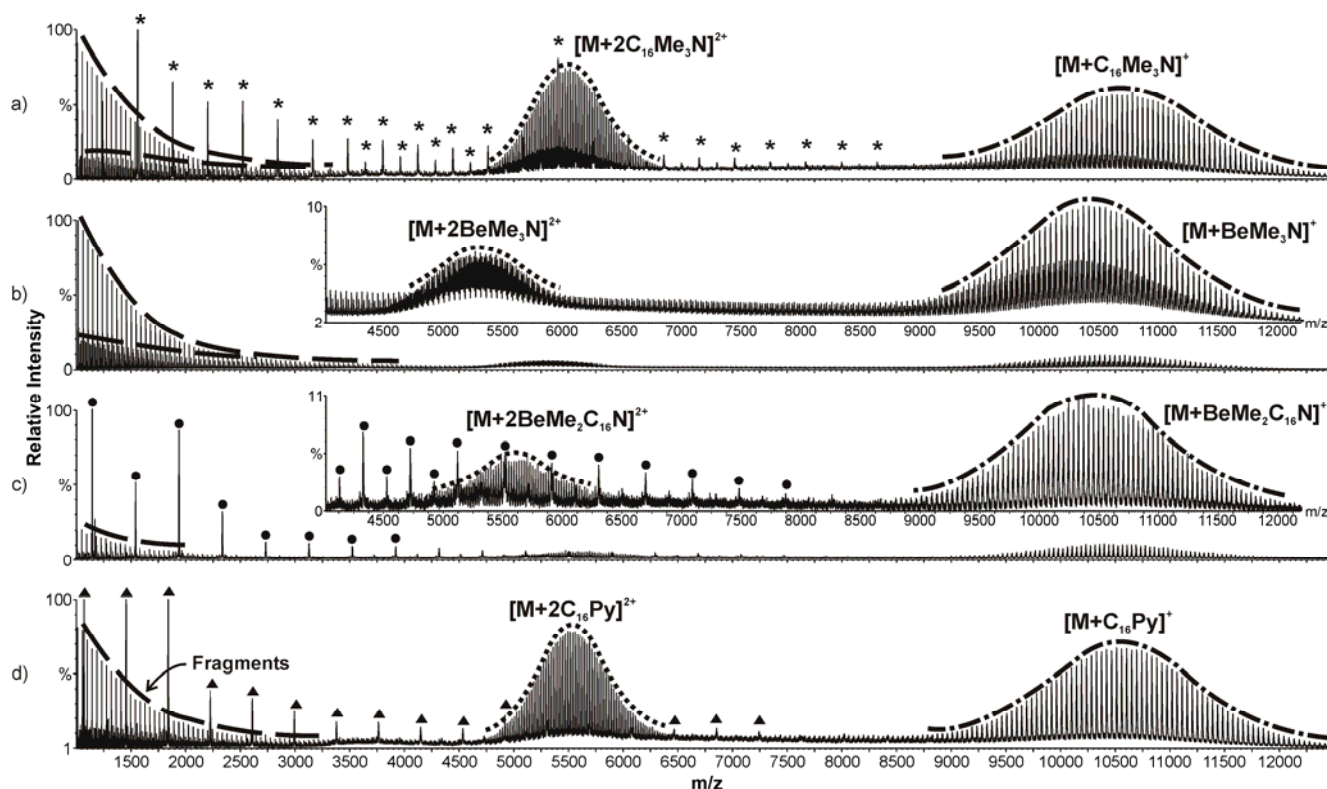


**Figure S-6.** Mass spectra of 10 kDa PEG obtained by direct infusion with addition of 1.2 mM of: a)  $C_{16}Me_3NCl$ , b)  $BeMe_3NCl$ , c)  $BeMe_2C_{16}NCl$ , and d)  $C_{16}PyBr$ . Note: Peaks indicated with an asterisk (\*), solid circle (●) and solid triangle (▲) are the respective Quat cluster ions. Inset figures are a magnification of the area of interest in Figures S-6b and S-6c.

$C_{16}PyBr$  has a comparable performance with  $C_{16}Me_3NCl$  in respect with the type and intensity of the formed low charge state ions. On the other hand,  $BeMe_3NCl$  and  $BeMe_2C_{16}NCl$  form low intensity low charge state ions. This behavior indicates that the Quats structure should be “bulky” enough to favorize the formation of low charge state ions but on the same time leave the ammonium’s positive charge accessible for coordination

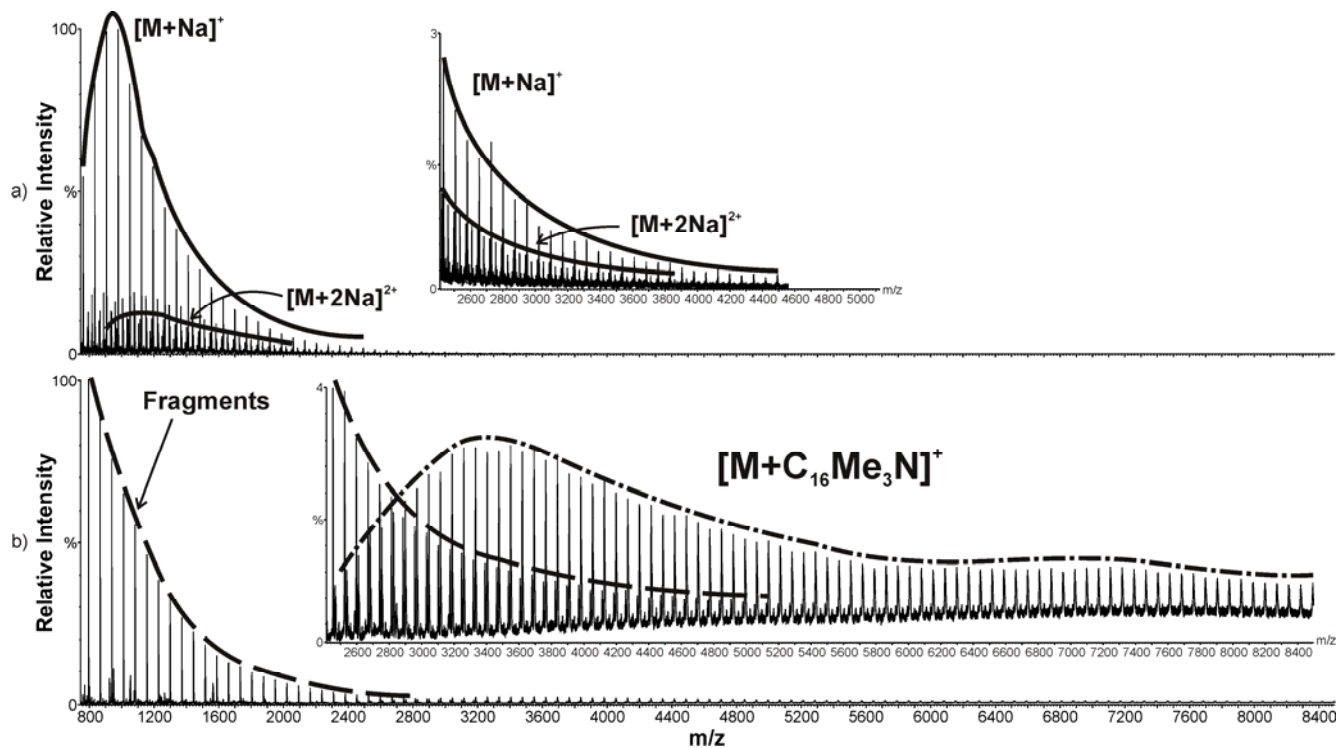


**Figure S-7.** DI-MS analysis of PTMEG 2.9 kDa. Summed spectra a) without addition of a Quat, and b) with addition of 1.2 mM  $C_{16}Me_3NCl$ . Note: Inset figures are a magnification of the area of interest in Figures S-7a and S-7b.



**Table S-1. Influence of the Quat concentration on the MWD as calculated from Figure 3**

Concentration <sup>a</sup> [uM]	$M_n - M_w^b$ [Da]	$M_n - M_w^c$ [Da]
0	4695 - 4735	ND
125	4863 - 4897	4852 - 4894
500	4922 - 4960	4833 - 4894
1000	ND	4943 - 4990
2000	ND	4974 - 5016

<sup>a</sup>Concentration of Quat in solution

<sup>b</sup> $M_n, M_w$  calculated from [PEG+2H]<sup>2+</sup> envelope

<sup>c</sup> $M_n, M_w$  calculated from [PEG+2C<sub>16</sub>Me<sub>3</sub>N]<sup>2+</sup> envelope.

By increasing the Quat concentration both envelopes seem shift to higher  $M_n, M_w$  values. Nevertheless the differences are within the error margin, hence cannot substantiate a specific trend

**Table S-2. Influence of the alkyl chain length on the MWD as calculated from Figure 4**

Quat	$M_n^a$	$M_w^a$
Me <sub>4</sub> NCl	10196	10234
C <sub>8</sub> Me <sub>3</sub> NCl	9984	10044
C <sub>12</sub> Me <sub>3</sub> NCl	10272	10323
C <sub>16</sub> Me <sub>3</sub> NCl	10078	10127

<sup>a</sup>The calculation of  $M_n, M_w$  was made using the doubly charge distribution with each Quat.

The results are within the error margin, hence not conclusive.